

When can hadronic loops scuttle the Okubo-Zweig-Iizuka rule?

Paul Geiger*

*Department of Physics, University of Toronto, Toronto, Canada M5S 1A7
and Continuous Electron Beam Accelerator Facility (CEBAF), 12000 Jefferson Avenue, Newport News, Virginia 23606*

Nathan Isgur

*Continuous Electron Beam Accelerator Facility (CEBAF), 12000 Jefferson Avenue, Newport News, Virginia 23606
(Received 21 September 1992)*

We have improved and extended our previous calculations of hadronic loop contributions to meson propagators. As we anticipated from our study of the vector mesons, systematic cancellations among the loops, which are crucial for the preservation of the Okubo-Zweig-Iizuka rule, continue to occur in all the low-lying nonets except 0^{++} . The failure of the cancellation mechanism in this sector has striking repercussions for the masses and couplings of the scalar mesons. We also present calculations of loop-induced SU(3) violation in the low-lying nonets.

PACS number(s): 12.40.Aa, 12.38.Aw, 13.25.+m, 14.40.-n

I. INTRODUCTION

Recently, we proposed a resolution to a longstanding and vexatious theoretical dilemma surrounding the Okubo-Zweig-Iizuka (OZI) rule [1, 2]. This dilemma, dubbed the “higher-order paradox” by Lipkin [3], emerges when one considers hadronic loop corrections to OZI-suppressed processes. Take, for example, $u\bar{u} \leftrightarrow d\bar{d}$ mixing in a vector meson propagator. The amplitude for such mixing, A , is directly measured by the ω - ρ mass splitting, and its smallness reflects the validity of the OZI rule: $m_\omega - m_\rho = 2A \sim 10$ MeV. Two time-orderings for this process are shown in Fig. 1, and though we may hypothesize that Fig. 1(a) is suppressed, Fig. 1(b) would seem to be large. It corresponds to a mesonic loop in the propagator (Fig. 2 makes this clearer), with strong-interaction vertices and a loop momentum that extends up to $\sim \Lambda_{\text{QCD}}$ (where it is cut off by the meson wave functions), so that this diagram must be expected to contribute $\sim \Lambda_{\text{QCD}}$ to OZI violation, i.e., to the ω - ρ mass splitting in this case. [Alternatively, we may note that the imaginary part of such a graph is a hadronic width. While small compared to typical hadronic masses (as expected from $N_c \rightarrow \infty$ arguments) typical widths are nonetheless large compared to 10 MeV.]

Our proposed resolution to the higher-order paradox, which we briefly recapitulate here, was based on the observation that the *sum* (over all two-meson intermediate states) of the “virtual-decay” diagrams in Fig. 2 can naturally be small, even though each individual diagram is indeed rather large. We pointed out that in fact there is a limit in which this sum is identically zero. To extract this limit, first note that the mixing amplitude corresponding to Fig. 2 is

$$A(E) = \sum_n \frac{\langle d\bar{d} | H_{\text{pc}}^{u\bar{u}} | n \rangle \langle n | H_{\text{pc}}^{d\bar{d}} | u\bar{u} \rangle}{(E - E_n)}, \quad (1)$$

where $H_{\text{pc}}^{f\bar{f}}$ is the quark pair creation operator for the flavor f and the set $\{|n\rangle\}$ is a complete set of two-meson intermediate states. In a *closure approximation*, in which the variation of the energy denominators associated with this sum is neglected, A is proportional to

$$B \equiv \sum_n \langle d\bar{d} | H_{\text{pc}}^{u\bar{u}} | n \rangle \langle n | H_{\text{pc}}^{d\bar{d}} | u\bar{u} \rangle = \langle d\bar{d} | H_{\text{pc}}^{u\bar{u}} H_{\text{pc}}^{d\bar{d}} | u\bar{u} \rangle, \quad (2)$$

and in the spectator approximation this further simplifies to

$$B = \langle d\bar{d} | H_{\text{pc}}^{d\bar{d}} | 0 \rangle \langle 0 | H_{\text{pc}}^{u\bar{u}} | u\bar{u} \rangle = |\langle d\bar{d} | H_{\text{pc}}^{d\bar{d}} | 0 \rangle|^2 = |\langle 0 | H_{\text{pc}}^{u\bar{u}} | u\bar{u} \rangle|^2; \quad (3)$$

thus we see that Fig. 2 will be suppressed whenever the created (destroyed) pair has only a small overlap with the final (initial) meson.

In Ref. [2] we argued that the approximations used to arrive at this suppression mechanism are not contrived, and in fact are well satisfied in what is currently the best-tested (and most successful) hadron decay model, the 3P_0 model [4, 5]. In this model the spectator approximation applies and the $q\bar{q}$ pairs are created and destroyed with 3P_0 quantum numbers so that, *except in the scalar meson sector*, they are orthogonal to the final and initial states.

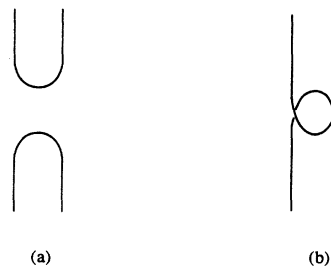


FIG. 1. A diagram associated with OZI violation shown in two time orderings.

*Present address: Physics Department, Carnegie Mellon University, Pittsburgh, PA 15213.

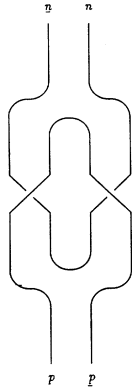


FIG. 2. OZI violation via two OZI-allowed amplitudes [a redrawing of Fig. 1(b)].

Furthermore, the severity of the closure approximation is mitigated because the cancellations that occur in the sum for B [Eq. (2)] occur between states with similar energy denominators. In our full calculation of Eq. (1) we indeed found $A \sim 10$ MeV, for a wide range of model parameters.

In this paper, we extend our calculations of $A(E)$ to all of the low-lying meson nonets [except the pseudoscalars which have a special status since η - η' mixing arises from the U(1) anomaly and there is no OZI rule to protect]. We also calculate the $u\bar{u} \leftrightarrow s\bar{s}$ mixing amplitudes

$$A'(E) \equiv \sum_n \frac{\langle s\bar{s} | H_{pc}^{u\bar{u}} | n \rangle \langle n | H_{pc}^{s\bar{s}} | u\bar{u} \rangle}{(E - E_n)}. \quad (4)$$

The physical significance of A and A' is most apparent when they are displayed as contributions to the meson mass matrix: in the flavor-diagonal $\{u\bar{u}, d\bar{d}, s\bar{s}\}$ basis the mass matrix may be written as

$$\begin{bmatrix} m + A & A & A' \\ A & m + A & A' \\ A' & A' & m + \Delta m + A'' \end{bmatrix}. \quad (5)$$

(A'' is the $s\bar{s} \leftrightarrow s\bar{s}$ mixing amplitude.) Note that $A' - A$ is an octet source of SU(3)-violation induced by the quark mass difference $\Delta m \equiv m_s - m_d$. Transforming to the ideally mixed basis $\{\frac{(u\bar{u}-d\bar{d})}{\sqrt{2}}, \frac{(u\bar{u}+d\bar{d})}{\sqrt{2}}, s\bar{s}\}$, the mass matrix becomes

$$\begin{bmatrix} m & 0 & 0 \\ 0 & m + 2A & \sqrt{2}A' \\ 0 & \sqrt{2}A' & m + \Delta m + A'' \end{bmatrix}, \quad (6)$$

and one sees that, in the almost ideally mixed nonets, $2A$ is the mass difference between the mostly nonstrange isoscalar meson and its isovector partner, and $\sqrt{2}A'/\Delta m$ is the mixing angle between the strange and nonstrange isoscalars.

In Sec. II below we will describe the ingredients of our calculations of A and A' , highlighting some differences in detail between our present and previous work. In Sec. III we discuss our findings, focusing especially on the scalar meson sector, where the loop graphs produce some extraordinary effects. Section IV contains our concluding remarks.

II. CALCULATING THE LOOPS

A. The 3P_0 decay model

Computation of the loop diagrams depicted in Fig. 2 is straightforward once the meson wave functions and the form of the (virtual) decay vertices are specified. Faced with the extremely large number of intermediate states in Eq. (1) (the principal, orbital, magnetic, and spin quantum numbers of both mesons, as well as the quantum numbers of their relative coordinate, must all be summed over), we have found it necessary to use harmonic oscillator wave functions. These are of course qualitatively similar to more realistic wave functions (e.g., Coulomb-plus-linear wave functions), and they give a tolerable account of the meson spectrum and its pattern of decay amplitudes (see for example Ref. [5]), but it would be desirable to dispense with this approximation in future calculations.

For the decay vertices, we employ a variant of the 3P_0 model. As mentioned above, this model has been thoroughly tested in studies of meson decays [4, 5]. Our present implementation of the 3P_0 model differs somewhat from the standard one (and, in one respect, from our own previous work in Ref. [2]). The classic 3P_0 model supposes that decays proceed by rearrangement of the quarks in the original hadron with a $q\bar{q}$ pair that is created out of the vacuum in a 3P_0 state. The pair creation is assumed to be pointlike and to occur with equal amplitude everywhere in space, leading to the following expression for an $A \rightarrow BC$ meson decay amplitude:

$$M(A \rightarrow BC) = (2\pi)^{3/2} \gamma_0 \phi \Sigma \cdot \int d^3k \Phi_B^*(\mathbf{k}) \Phi_C^*(\mathbf{k})(2\mathbf{k} + \mathbf{q}) \times \Phi_A\left(\mathbf{k} - \frac{\mathbf{q}}{2}\right), \quad (7)$$

where the Φ 's are momentum-space meson wave functions, \mathbf{q} is the momentum of meson B , ϕ is a flavor overlap, Σ is a spin overlap, and γ_0 , the intrinsic pair creation strength, is the only parameter of the model. The latter is fixed by fitting Eq. (7) to a measured decay width. Three modifications of the simple 3P_0 model are required for our purposes.

(i) *Inclusion of a string-overlap factor.* We employ the flux tube picture of Refs. [5] and [6], wherein the decay vertices of Fig. 2 arise from the breaking of a chromoelectric flux tube that joins the initial quark and antiquark. The pair is thus created in a finite region defined by the overlap of the initial and final string wave functions. In Ref. [5] it was shown that this overlap function has the approximate form

$$\tilde{\Psi}(\mathbf{r}, \mathbf{w}) = e^{-\frac{1}{2}w_{\perp}^2}, \quad (8)$$

where b is the string tension, the coordinates \mathbf{r} and \mathbf{w} are defined in Fig. 3(a), and w_{\perp} is the component of \mathbf{w} perpendicular to \mathbf{r} . Here we mock up $\tilde{\Psi}(\mathbf{r}, \mathbf{w})$ with a sum of staggered Gaussians [see Fig. 3(b)]:

$$\tilde{\Psi}(\mathbf{r}, \mathbf{w}) = \frac{1}{2g+1} \sum_{n=-g}^g \exp\left[-\frac{b}{2}\left(\mathbf{w} + \frac{n}{2g}\mathbf{r}\right)^2\right]. \quad (9)$$

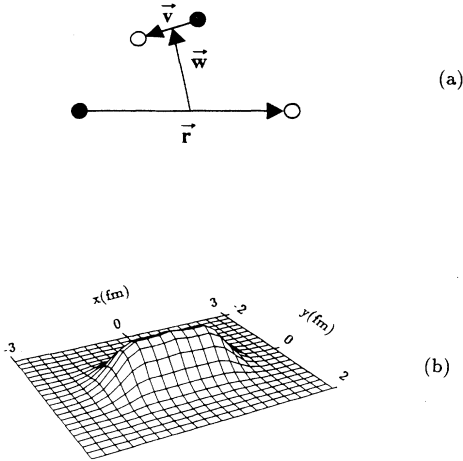


FIG. 3. (a) Position space coordinates for meson decay by pair creation. (b) The amplitude for pair creation in the region surrounding a fixed quark and antiquark [at $(x,y) = (-1,0)$ and $(1,0)$, respectively]. This function, obtained from Eq. (9) with $g = 1$, closely approximates the cigar-shaped function advocated in Ref. [5].

In Ref. [2] we used a simpler, spherical form for $\tilde{\Psi}$, but this is not adequate for our present calculations because it “artificially” causes the closure sum to vanish identically for even-parity initial states—see Sec. II B.

(ii) *Form factor for pair creation.* It is appropriate in a constituent model to replace the pointlike pair creation operator $q^\dagger(\mathbf{r})\boldsymbol{\alpha} \cdot \nabla q(\mathbf{r})$ with a nonlocal operator, which

we take to have the form

$$H_{pc} = \left(\frac{3}{8\pi r_q^2}\right)^{3/2} \int d^3u q^\dagger\left(\mathbf{r} + \frac{\mathbf{u}}{2}\right) \times e^{-\frac{3u^2}{8r_q^2}} \boldsymbol{\alpha} \cdot \nabla q\left(\mathbf{r} - \frac{\mathbf{u}}{2}\right). \quad (10)$$

This operator creates the pair with a mean separation of order the “constituent quark size,” r_q . In addition to being well-motivated physically, this nonlocality renders finite the sum over the complete set of virtual decay channels. As discussed in [2], the value of r_q is constrained by meson decay data.

(iii) *Suppression of pair creation at short distances.* Pair creation occurs in the chromoelectric field between the initial quark and antiquark. As the distance r between these sources approaches zero, the field vanishes and so does the amplitude for pair creation. In our previous calculations with 1^{--} initial states, it was plausible to ignore this short-distance effect. It is, however, potentially very important in the 0^{++} sector: since the initial-state $q\bar{q}$ pair must be rather close together ($r \lesssim r_q$) in order to be annihilated by H_{pc} , weakening H_{pc} at small r may significantly reduce the otherwise unsuppressed 0^{++} closure sum. We incorporate this effect by multiplying H_{pc} by $(1 - e^{-tbr^2})$. This physically reasonable functional form allows us to perform some of our computations analytically. The parameter t controls the onset of short distance suppression; we shall find that our results are not strongly t dependent.

Combining the above three ingredients, we obtain the following generalization of Eq. (7):

$$M(A \rightarrow BC) = \frac{2}{(2\pi)^{3/2}} \gamma_0 \phi \Sigma \cdot \int d^3k d^3p d^3p' \Psi(\mathbf{p}, \mathbf{p}') \Phi_B^* \left(\mathbf{k} + \frac{\mathbf{p}'}{2}\right) \Phi_C^* \left(\mathbf{k} - \frac{\mathbf{p}'}{2}\right) \times \left(\mathbf{k} + \frac{\mathbf{q}}{2}\right) \exp\left[-\frac{2r_q^2}{3} \left(\mathbf{k} + \frac{\mathbf{q}}{2}\right)^2\right] \Phi_A \left(\mathbf{k} - \frac{\mathbf{q}}{2} - \mathbf{p}\right), \quad (11)$$

where $\Psi(\mathbf{p}, \mathbf{p}')$ is the Fourier transform of $(1 - e^{-tbr^2})\tilde{\Psi}(\mathbf{r}, \mathbf{w})$. With our model thus completely specified, we can proceed to calculate the loop diagrams.

B. Results

One of the main lessons of Ref. [2] was that the magnitude of $A(E)$ is essentially controlled by the value of the

closure sum, B ; the energy denominators in Eq. (1) do not significantly alter the relative signs and magnitudes of the terms in Eq. (2). Thus, with the expectation that $A(E)$ will be of order B/E_{typ} , where $E_{\text{typ}} \sim 1$ GeV is a typical energy denominator, we begin by calculating closure sums. The general formula is

$$B = \delta_{S,1} \gamma_0^2 \beta^2 \int d^3w \left| \sum_m \langle 1, 1, m, -m | 0, 0 \rangle \langle \ell, S, M+m, -m | J, M \rangle \times \int d^3r (1 - e^{-tbr^2}) \tilde{\Psi}(\mathbf{r}, \mathbf{w}) \psi_A^{\ell, M+m}(\mathbf{r}) \psi_P^{*1, m}(\mathbf{r}) \right|^2, \quad (12)$$

where $\psi_A^{\ell m}$ is the spatial wave function of the initial meson (with harmonic oscillator parameter β), S is its total quark spin, $\psi_P^{\ell m}$ is the wave function of the created pair, and $\langle j_1 j_2 m_1 m_2 | JM \rangle$ is a Clebsch-Gordan coefficient. This equation shows that B vanishes identically

in odd-parity nonets (where ℓ_A is even), and in nonets with total quark spin zero (because the pair creation operator has total quark spin one). It turns out that B vanishes in the 3P_1 nonet as well, due to an “accidental” selection rule. In the 3P_2 and 3F_4 nonets, B is nonzero

because the nonsphericity of the string-overlap function $\tilde{\Psi}(\mathbf{r}, \mathbf{w})$ effectively violates the spectator approximation. Figure 4 shows the 3P_2 and 3P_0 closure sums as functions of r_q and t . We do not show the 3F_4 closure sum, as it is extremely small (less than 10^{-4} GeV² over the whole range of our parameters).

Observe that the closure sum is quite small in the 3P_2 sector; the string-overlap function does not badly spoil the spectator approximation. On the other hand, B tends to be very large in the 3P_0 sector. Though the short-distance suppression factor $(1 - e^{-tbr^2})$ causes B to vanish when $r_q = 0$ as expected, B rises very rapidly as r_q is increased. Beyond $r_q = 0.1$ fm (which is perhaps its minimum reasonable value) the closure result is large. One reason for the failure of the short-distance suppression factor to completely subdue the closure sum is that any overall weakening of the pair creation operator H_{pc} must be compensated by an increase in γ_0 , in order to fit the meson decay data. [In particular, $\gamma_0(1 - e^{-tbr^2})$ goes to a nonzero limit as $t \rightarrow 0$.]

With our expectations thus primed by Fig. 4, we turn to the actual calculation of $A(E)$. Performing the sum in Eq. (1) is a numerical challenge; in order to see good convergence, we have found it necessary to sum over intermediate-state mesons with up to ≈ 4 units of radial excitation and ≈ 9 units of orbital excitation. This translates into $\sim 10^4$ terms overall. Appendix I details some of the calculational techniques we used to compute these terms efficiently, and Appendix II discusses some finer details of the sum, especially the tendency of neighboring terms to cancel. Our results are shown in Tables I and II [7].

Referring first to Table I, we see that our closure limit findings were not misleading; A is uniformly small except in the scalar nonets (which we will discuss in Sec. III), and this qualitative result is stable under all reasonable parameter variations. This is our first main conclusion: the closure mechanism suppresses loop corrections in all of the low-lying sectors except 0^{++} . (In Ref. [2] we calculated A only in the vector nonet.) While we do not expect our calculations to accurately predict the experimental mixing amplitudes, both because of the rather delicate cancellations that occur among the loop diagrams and because we have neglected some potentially important physics [such as “pure annihilation” through

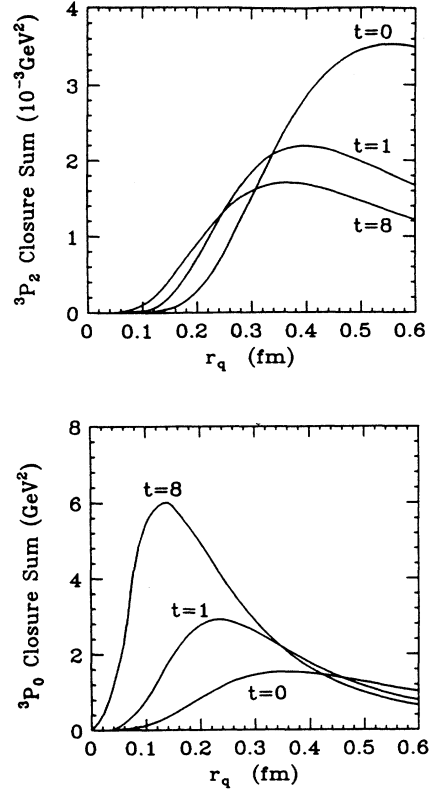


FIG. 4. Closure sums of Eq. (12), for the 3P_2 and 3P_0 nonets, shown as functions of the pair creation form factor, r_q , and the short-distance suppression parameter, t .

gluons as shown in Fig. 1(a), and interactions between the intermediate-state mesons], it is nevertheless interesting to compare our results to the experimental values shown in the final column of Table I. We can draw no definite conclusions about the signs of our 3S_1 and 3D_3 amplitudes, since they are sensitive to parameter changes. Note, however, that 3S_1 generally comes out as the smallest calculated amplitude, and it is also probably the smallest measured amplitude. (3F_4 is also small, but with large error bars.) In the 1P_1 , 3P_1 , 3P_2 , and 3F_4 nonets the calculated signs are stable, and only 3P_2 is in disagreement with the data. We consistently obtain a

TABLE I. Hadronic loop contributions to the mixing amplitudes $A(u\bar{u} \leftrightarrow d\bar{d})$. In the almost-ideally-mixed nonets, $2A$ is the (nonstrange-) isoscalar-isovector mass splitting. Entries are in MeV, and our “standard parameters” are $\beta = 0.4$ GeV, $b = 0.18$ GeV², $r_q = 0.30$ fm, $g = t = 1$.

Nonet	Standard parameters	$r_q = 0.25$ fm	$\beta = 0.3$ GeV	$b = 0.24$ GeV ²	$t = 1/2$	$g = 1/2$	Expt
3S_1	-2.0	2.2	-1.1	-4.3	0.3	-2.2	7 ± 1
1P_1	-15.0	-22.3	-15.8	-15.2	-12.9	-15.9	-32 ± 12
3P_2	6.2	0.5	19.7	5.1	8.9	3.9	-22 ± 3
3P_1	12.4	23.9	13.9	15.0	6.5	15.6	11 ± 15
3D_3	3.6	2.9	-3.8	3.1	4.3	3.2	-12 ± 4
3F_4	15.6	14.5	10.3	13.4	22.1	12.2	6 ± 18
3P_0	-459	-528	-254	-431	-422	-597	see text
$2{}^3P_0$	-63	-135	-96	-58	-92	-60	see text

TABLE II. Hadronic loop contributions to the mixing amplitudes, $A'(u\bar{u} \leftrightarrow s\bar{s})$. For reference, we also show the corresponding amplitude, A , from Table I. Entries are in MeV and our standard parameters were used.

	$A(m_{n_s})$	$A'(m_{s\bar{s}})$	$A'(m_{n_s})$
3S_1	-2.0	8.6	-4.2
1P_1	-15.0	-59.4	-47.4
3P_2	6.2	-7.1	-18.7
3P_1	12.4	89.5	91.6
3D_3	3.6	7.4	2.4
3F_4	15.6	11.2	-0.8
3P_0	-459	-537	-572
2^3P_0	-63	-89	-61

relatively large 1P_1 amplitude, and the measured value is also relatively large. Surprisingly, the calculated A 's are, on the whole, in fair quantitative agreement with the data, suggesting that the hadronic loop diagrams may be the dominant source of mixing.

The $u\bar{u}$ (or $d\bar{d}$) $\leftrightarrow s\bar{s}$ mixing amplitudes $A'(E)$, defined in Eq. (4), are shown in Table II. Recall that $A'(E)$ measures the amount of ϕ - ω mixing in the vector sector, f_2 - f_2' mixing in the tensor sector, etc. For each parameter set, we show both $A'(m_{s\bar{s}})$ and $A'(m_{n_s})$ ($m_{s\bar{s}}$ is the mass of the mostly- $s\bar{s}$ isoscalar and m_{n_s} is the mass of its mostly nonstrange partner). These two amplitudes are in general different, reflecting the fact that (for example) the amount of ω in the ϕ is not necessarily the same as the amount of ϕ in ω once we admit more than just valence quarks into the mesonic wave functions. From the perspective of SU(3) symmetry, these effects are very mild. If we write, for example

$$\begin{aligned}\omega &= \omega_1 \cos \theta + \omega_8 \sin \theta, \\ \phi &= -\omega_8 \cos \theta + \omega_1 \sin \theta,\end{aligned}$$

then $\theta \approx \theta_{\text{ideal}} \approx 35.3^\circ$, but it deviates from this value at m_ω and m_ϕ by angles ϕ_ω and ϕ_ϕ which are both small ($\lesssim 5^\circ$), so that SU(3) breaking is small. However, our calculation shows that $(\phi_\omega - \phi_\phi)/(\phi_\omega + \phi_\phi)$ can be of order unity, so that deviations from ideal mixing can be very different in the ω and ϕ . Thus there seems to be little reason to expect that OZI violation in, e.g., $\phi \rightarrow \rho\pi$ or $\phi \rightarrow \pi\gamma$, arising from $A'(m_\phi)$, can be quantitatively correlated with $m_\omega - m_\rho$, which arises from $A(m_\omega)$.

In the 3S_1 , 3P_2 , 3D_3 , and 3F_4 nonets, the loop graphs produce only a small deviation from ideal mixing: $|A'| \sim 10$ MeV. However, the 1P_1 and 3P_1 nonets, where $|A'| \gtrsim 50$ MeV, are more interesting. The relatively large amplitudes in these sectors are a consequence of nearby S -wave threshold effects: h_1' and f_1' are within ≈ 100 MeV of $K^*\bar{K}$ threshold, while f_2' , for example, is 270 MeV from its corresponding $K^*\bar{K}^*$ threshold. (Of course, in the vector sector ϕ is very close to $K\bar{K}$ threshold, but there the coupling is P wave and hence rather weak.) A mixing amplitude of 50 MeV corresponds to a deviation from ideal mixing of approximately 10° . This should have observable effects on the decay branching ratios of h_1, h_1' and f_1, f_1' ; unfortunately, the data on these states is presently too sparse to check this.

III. THE SCALAR SECTOR

Our most striking results are contained in the final two rows of Tables I and II. Both in the closure limit and in the full calculation, we find that hadronic loops lead to extremely large OZI-violating mixing amplitudes in the scalar mesons: $A, A' \sim -500$ MeV for 1^3P_0 (and ~ -100 MeV for 2^3P_0).

Large values for A and A' imply large isoscalar-isovector mass splittings, and large deviations from ideal mixing. It is difficult to accurately quantify these statements because the scalar meson sector, even in the absence of loop effects, is exceptionally complex: the lightest glueball is expected to appear at ≈ 1.5 GeV [9], the observed states near $K\bar{K}$ threshold are apparently exotic objects, probably $K\bar{K}$ molecules [10], and S -wave pseudoscalar-pseudoscalar channels like $\pi\pi, K\bar{K}$, etc., which dominate the low-energy intermediate states of Fig. 2, are known to have very strong final-state interactions. Given these complexities, the only firm conclusion we can now draw is that we expect the scalar meson sector to behave with respect to the OZI rule in a dramatically different fashion from any other sector, and hence that a full coupled channel analysis of the scalars is worth pursuing.

In the meantime, we would like to outline a rough scenario, which neglects all of the complications just mentioned, and compare it with what is known experimentally. Returning to the mass matrix of Eq. (5), we suppose that in the absence of loop effects the scalars are split from the other P waves by a small spin-orbit coupling; we thus adopt the nominal masses $m = 1200$ MeV and $m + \Delta m = 1450$ MeV. Also, since the differences between A and A' are rather small (on the scale of A), for the sake of simplicity we set $A' = A'' = A$. Then, upon diagonalizing the mass matrix, we find that the isovector of course remains at 1200 MeV, while the isoscalar masses vary with A as follows:

$$\begin{aligned}A = -100 \text{ MeV} &\Rightarrow m = 950 \text{ MeV and } 1400 \text{ MeV,} \\ A = -200 \text{ MeV} &\Rightarrow m = 660 \text{ MeV and } 1390 \text{ MeV,} \\ A = -300 \text{ MeV} &\Rightarrow m = 370 \text{ MeV and } 1380 \text{ MeV.}\end{aligned}$$

In each case, the low mass eigenstate f_0^L is rotated away from $\frac{(u\bar{u}+d\bar{d})}{\sqrt{2}}$ flavor composition towards the flavor-singlet state, while the high mass state f_0^H moves from $s\bar{s}$ towards $(-1\times)$ flavor-octet. The rotation to the octet-singlet basis is essentially complete for $-A \geq 250$ MeV.

Thus, in this naive scenario, we see that the loop diagrams would produce a drastic distortion of the usual quark model picture of the scalar meson sector, and lead us to predict a low-mass ($m_L = 500$ – 1000 MeV) state with approximately flavor singlet couplings, together with an approximately flavor-octet state with mass $m_H \approx 1400$ MeV. The widths of these states, calculated in the flux tube model of Ref. [5] are $\Gamma_L = 200$ – 500 MeV and $\Gamma_H = 150$ MeV, respectively. The mass m_L and also the width Γ_L (through its dependence on the available phase space) are strongly dependent on A , but our perturbative calculation cannot be trusted to give an accurate value for this quantity. We can only

conclude with certainty that A is large. On the other hand, m_H varies only slightly with A , and our estimate of its width is probably reliable to within a factor of 2. (This being the intrinsic accuracy of the flux tube decay model.)

The f_0^H may be the observed $f_0(1400)$, which has a measured width of 150–400 MeV [11]. (The calculated width assuming $\frac{(u\bar{u}+d\bar{d})}{\sqrt{2}}$ flavor composition is 450 MeV.) By an unhappy coincidence, the $\pi\pi : K\bar{K} : \eta\eta$ branching ratios are the same for $\frac{(u\bar{u}+d\bar{d})}{\sqrt{2}}$ and flavor octet assignments, so it is difficult to distinguish between these two alternatives.

There are also some experimental indications of a scalar meson in the 700–900 MeV mass region. For example, the coupled-channel analysis of Au *et al.* [13] found a broad isoscalar scalar at 910 MeV with $\Gamma \approx 700$ MeV. Their state couples to $\pi\pi$ about twice as strongly as it does to $K\bar{K}$. See Refs. [11,12] for a discussion of this region and for further references.

The loop graphs would have similar, though less pronounced, effects on the radial recurrences of the $q\bar{q}$ scalar mesons, moving them from ≈ 1.8 and 2.0 GeV to ≈ 1.5 –1.7 and 1.95 GeV, respectively, and rotating the flavor wave functions about halfway towards the octet-singlet basis. The former state may be the $f_0(1710)$.

It is interesting (and unsettling) that even this naive scenario is not yet ruled out. We cannot anticipate the conclusions of a more comprehensive analysis, but we offer two comments: (1) The strong attractive $\pi\pi$ interaction at low mass will tend to raise the mass of f_0^L and make it broader, and (2) The interaction of these states with the $f_0(975)$ could be important; for example, Ref. [10] found that the $f_0(1400)$ was essential in producing the interaction which bound the $K\bar{K}$ molecule.

IV. CONCLUSIONS AND OUTLOOK

We have tested our proposed explanation for the anomalous absence of strong loop corrections in meson propagators, and found it to be viable: except in the scalar nonets, 3P_0 dominance of the effective pair creation operator causes the sum of all loop diagrams to vanish in the closure and spectator approximations. Furthermore, in a realistic model which incorporates departures from these approximations, the loops continue to cancel to a great extent.

However, in the scalar meson sector, the cancellation mechanism breaks down spectacularly, leading us to predict very large OZI-violating loop effects which are expected to manifest themselves as large shifts in the masses and mixing angles of the scalar mesons: the initially nonstrange 0^{++} isoscalar could well appear several hundred MeV below the naive quark model estimate, with approximately flavor singlet couplings, while the initially $s\bar{s}$ state suffers an associated downward shift of ≈ 50 MeV, ending up with an approximately flavor-octet composition. Similar but subdued effects would in this scenario be expected for the radial recurrences of these states. The experimental situation is very unclear, but it appears not to be in contradiction with this naive picture. Nevertheless, there are many complexities in the scalar meson sector, so that considerable further study is required before any definite conclusions can be drawn.

In addition to such studies, we hope in the future to extend our calculations to baryon two-point functions, and then to general three-point functions, where the effects of the virtual hadronic loops may be seen more directly by external probes.

ACKNOWLEDGMENTS

N.I. would like to thank Sidney Coleman for stressing the potential importance of color screening at short distances. P.G. would like to thank the CEBAF Theory Group for its hospitality and financial support during the period when this work was completed. This work was supported in part by the Natural Sciences and Engineering Research Council of Canada and by the U.S. Department of Energy under contract DE-AC05-84ER40150.

APPENDIX A: CALCULATIONAL TECHNIQUES

In order to accurately sum the large number of loop diagrams that contribute to each meson propagator, we required a very fast and accurate technique for computing 3P_0 overlap integrals. The method we settled upon entails working in rectangular coordinates, where the overlap integrals separate and, more importantly, satisfy recursion relations.

The overlap integral appearing in Eq. (11) may be written as

$$\begin{aligned} \bar{I}_{ABC} &= \sum_{n=-g}^g \frac{b^{-3/2}}{2g+1} \int d^3u d^3v d^3w \left\{ \delta^3 \left[\mathbf{w} + \frac{n}{2g}(\mathbf{u}-\mathbf{v}) \right] - \frac{\exp \left[\frac{-1}{4tb} \left(\mathbf{w} + \frac{n}{2g}(\mathbf{u}-\mathbf{v}) \right)^2 \right]}{(4\pi tb)^{3/2}} \right\} \\ &\times \exp \left[-\frac{(\mathbf{u}-\mathbf{v})^2}{2b} \right] \exp \left[-\frac{r_q^2}{6} (\mathbf{u} + \mathbf{v} + \mathbf{q})^2 \right] (\mathbf{u} + \mathbf{v} + \mathbf{q}) \\ &\times \Phi_B^*(\mathbf{u}) \Phi_C^*(\mathbf{v}) \Phi_A \left(\frac{\mathbf{u} + \mathbf{v} - 2\mathbf{w} - \mathbf{q}}{2} \right) \\ &\equiv \sum_{n=-g}^g \left\{ \bar{I}(n, 0) - \bar{I}(n, t) \right\}. \end{aligned} \quad (\text{A1})$$

(We have set the harmonic oscillator parameter, β , equal to 1.) If we work in a basis of rectangular harmonic oscillator wave functions $\Phi_{A_x A_y A_z}$, etc., then the x , y , and z integrations separate:

$$(-i)^{N_B+N_C-N_A} \vec{I}(n, t) = \frac{1}{2g+1} \begin{pmatrix} i'_{A_x B_x C_x} & i_{A_y B_y C_y} & j_{A_z B_z C_z} \\ i_{A_x B_x C_x} & i'_{A_y B_y C_y} & j_{A_z B_z C_z} \\ i_{A_x B_x C_x} & i_{A_y B_y C_y} & j'_{A_z B_z C_z} \end{pmatrix}, \quad (\text{A2})$$

where $N_A \equiv A_x + A_y + A_z$, etc., and we have introduced a set of four basic three-dimensional integrals,

$$i_{ABC} \equiv \frac{\eta_A \eta_B \eta_C}{\sqrt{4\pi t b^2}} \int du dv dw e^{-\frac{1}{4tb}[w+\frac{n}{2g}(u-v)]^2 - \frac{1}{2b}(u-v)^2 - \frac{r^2}{6}(u+v)^2 - \frac{1}{2}(u^2+v^2) - \frac{1}{8}(u+v-2w)^2} \\ \times H_B(u) H_C(v) H_A\left(\frac{u+v-2w}{2}\right), \quad (\text{A3})$$

$$i'_{ABC} \equiv \frac{\eta_A \eta_B \eta_C}{\sqrt{4\pi t b^2}} \int du dv dw e^{-\frac{1}{4tb}[w+\frac{n}{2g}(u-v)]^2 - \frac{1}{2b}(u-v)^2 - \frac{r^2}{6}(u+v)^2 - \frac{1}{2}(u^2+v^2) - \frac{1}{8}(u+v-2w)^2} \\ \times H_B(u) H_C(v) H_A\left(\frac{u+v-2w}{2}\right) (u+v), \quad (\text{A4})$$

$$j_{ABC} \equiv \frac{\eta_A \eta_B \eta_C}{\sqrt{4\pi t b^2}} \int du dv dw e^{-\frac{1}{4tb}[w+\frac{n}{2g}(u-v)]^2 - \frac{1}{2b}(u-v)^2 - \frac{r^2}{6}(u+v+q)^2 - \frac{1}{2}(u^2+v^2) - \frac{1}{8}(u+v-2w-q)^2} \\ \times H_B(u) H_C(v) H_A\left(\frac{u+v-2w-q}{2}\right), \quad (\text{A5})$$

$$j'_{ABC} \equiv \frac{\eta_A \eta_B \eta_C}{\sqrt{4\pi t b^2}} \int du dv dw e^{-\frac{1}{4tb}[w+\frac{n}{2g}(u-v)]^2 - \frac{1}{2b}(u-v)^2 - \frac{r^2}{6}(u+v+q)^2 - \frac{1}{2}(u^2+v^2) - \frac{1}{8}(u+v-2w-q)^2} \\ \times H_B(u) H_C(v) H_A\left(\frac{u+v-2w-q}{2}\right) (u+v+q). \quad (\text{A6})$$

Here the H 's are Hermite polynomials, $\mathbf{q} = q\hat{\mathbf{z}}$, and the η 's are normalization constants given by $\eta_j \equiv (\pi^{1/2} 2^j j!)^{-1/2}$. Because the Hermite polynomials satisfy recursion relations,

$$H_{n+1}(x) - 2xH_n(x) + 2nH_{n-1}(x) = 0 \quad (\text{A7})$$

and

$$\frac{dH_n(x)}{dx} - 2nH_{n-1}(x) = 0, \quad (\text{A8})$$

it is possible to show that the i 's and j 's may themselves be obtained recursively:

$$i_{0BC} = \sqrt{\frac{C-1}{C}} k_1 i_{0BC-2} - \sqrt{\frac{B}{C}} k_2 i_{0B-1C-1} \\ = \sqrt{\frac{B-1}{B}} k_3 i_{0B-2C} - \sqrt{\frac{C}{B}} k_4 i_{0B-1C-1}, \quad (\text{A9})$$

$$i_{ABC} = \sqrt{\frac{C+1}{A}} k_5 i_{A-1BC+1} + \sqrt{\frac{C}{A}} k_6 i_{A-1BC-1} - \sqrt{\frac{A-1}{A}} k_7 i_{A-2BC}, \quad (\text{A10})$$

and similarly, for the j 's,

$$j_{0BC} = \sqrt{\frac{C-1}{C}} k_1 j_{0BC-2} - \sqrt{\frac{B}{C}} k_2 j_{0B-1C-1} + \sqrt{\frac{2}{C}} q k_8 j_{0BC-1} \\ = \sqrt{\frac{B-1}{B}} k_3 j_{0B-2C} - \sqrt{\frac{C}{B}} k_4 j_{0B-1C-1} + \sqrt{\frac{2}{B}} q k_9 j_{0B-1C}, \quad (\text{A11})$$

$$j_{ABC} = \sqrt{\frac{C+1}{A}} k_5 j_{A-1BC+1} + \sqrt{\frac{C}{A}} k_6 j_{A-1BC-1} \\ - \sqrt{\frac{A-1}{A}} k_7 j_{A-2BC} + \sqrt{\frac{2}{A}} q k_{10} j_{A-1BC}. \quad (\text{A12})$$

The recursion constants k_1 through k_{10} may be written in terms of

$$D_1 \equiv \left(\frac{3}{b} + \frac{3}{2} + \frac{n^2}{2g^2} \right) + \frac{r_q^2}{3} \left(2 + \frac{4}{b} + \frac{n^2}{g^2} \right) + t(2+b) \left(\frac{4}{3} r_q^2 + 2 \right) \quad (\text{A13})$$

and

$$D_2 \equiv \left(\frac{1}{4} - \frac{1}{b} - \frac{n^2}{4g^2} + \frac{r_q^2}{3} \right) + 2t \left(\frac{br_q^2}{3} - 1 \right) \quad (\text{A14})$$

as follows:

$$k_1 = \frac{1}{D_1} \left[\left(1 - \frac{1}{b} + \frac{n}{g} \right) - \frac{r_q^2}{3} \left(\frac{4}{b} + \frac{n^2}{g^2} \right) + 2t \left(b - \frac{4}{3} r_q^2 \right) \right], \quad (\text{A15})$$

$$k_2 = k_4 = \frac{1}{D_1} \left[\left(\frac{1}{2} - \frac{2}{b} - \frac{n^2}{2g^2} \right) + \frac{2}{3} r_q^2 + 4t \left(\frac{br_q^2}{3} - 1 \right) \right], \quad (\text{A16})$$

$$k_3 = k_1 - \frac{2n}{D_1 g}, \quad (\text{A17})$$

$$k_5 = \frac{1}{D_2} \left[\left(-\frac{1}{2} - \frac{1}{b} - \frac{n}{2g} - \frac{nr_q^2}{3g} \right) \right], \quad (\text{A18})$$

$$k_6 = k_5 + \frac{1}{D_2} \left[1 + \frac{n}{g} \right] \quad (\text{A19})$$

$$k_7 = \frac{1}{D_2} \left[\left(-\frac{1}{4} - \frac{1}{b} + \frac{n^2}{4g^2} + \frac{r_q^2}{3} \right) - 2t \left(\frac{br_q^2}{3} - 1 \right) \right], \quad (\text{A20})$$

TABLE III. Individual contributions to A in the 3P_2 sector, from some low-lying intermediate states. The terms are grouped by $N \equiv n_b + n_c$ and $L \equiv \ell_b + \ell_c + \ell_{\text{rel}}$, and within each group they are labeled by $(\ell_b \ell_c \ell_{\text{rel}})$. Note the tendency for the terms to cancel locally. (Entries are in MeV, and our standard parameters were used.)

	$L=0$		$L=2$		$L=4$	
$N=0$	(0 0 0):	-30.2	(0 0 2):	23.6	(1 0 3):	0.7
			(1 0 1):	62.5	(1 1 2):	-6.3
			(1 1 0):	-34.6	(2 0 2):	-5.1
			(2 0 0):	0.5	(2 1 1):	17.3
					(2 2 0):	-6.0
	total:	-30.2	total:	52.0	(3 0 1):	0.3
				(3 1 0):	-1.4	
				total:	-0.5	
$N=1$	(0 0 0):	-15.0	(0 0 2):	-0.2	(1 0 3):	0.1
			(1 0 1):	5.1	(1 1 2):	-0.5
			(1 1 0):	-1.8	(2 0 2):	-1.5
			(2 0 0):	-0.7	(2 1 1):	2.0
					(2 2 0):	-0.1
	total:	-15.0	total:	2.4	(3 0 1):	0.1
				(3 1 0):	-0.2	
				total:	-0.1	
$N=2$	(0 0 0):	-1.5	(0 0 2):	0.0	All less than 1 MeV	
			(1 0 1):	0.9		
			(1 1 0):	-0.3		
			(2 0 0):	0.0		
	total:	-1.5	total:	0.6	total:	0.1

$$k_8 = \frac{1}{D_1} \left[\left(\frac{1}{4} + \frac{1}{2b} - \frac{n}{4g} \right) - \frac{r_q^2}{3} \left(1 + \frac{2}{b} + \frac{n}{g} + \frac{n^2}{2g^2} \right) - 2t \frac{r_q^2}{3} (2+b) \right], \quad (\text{A21})$$

$$k_9 = k_8 + \frac{1}{D_1} \left[\frac{n}{2g} + \frac{2nr_q^2}{3g} \right], \quad (\text{A22})$$

$$k_{10} = \frac{1}{D_2} \left[\frac{1}{2b} - \frac{r_q^2}{3} \left(1 + \frac{n}{2g} \right) \right]. \quad (\text{A23})$$

The recursion technique allows the i 's and j 's to be obtained very rapidly. The transformation back to the spherical basis via

$$|n \ell m\rangle = \sum_{n_x n_y n_z} |n_x n_y n_z\rangle \langle n_x n_y n_z | n \ell m\rangle \quad (\text{A24})$$

is straightforward. Note finally that, by virtue of Eqs. (A7) and (A8), the i 's and j 's are simple linear combinations of the i 's and j 's.

APPENDIX B: MAGIC LIMITS

In Ref. [2] we discussed at length the cancellations that occur in the closure sum. We showed that not only does the sum over *all* intermediate states vanish, but in fact many subcancellations occur. Moreover, these subcancellations are among states with similar energies, so that they tend to be preserved even in the full calculation with energy denominators.

Specifically, for a “magic” value of r_q , namely $r_q = \frac{\sqrt{3}}{2\beta}$, the overlap integrals simplify greatly and it was possible to show that each subset of terms with a given value of $2(n_b + n_c) + (\ell_b + \ell_c + \ell_{\text{rel}}) \equiv 2N + L$ sums to zero. (Thus, for example, intermediate states containing two S -wave mesons in a relative P wave exactly cancel with intermediate states where an S -wave meson and a P -wave meson are in a relative S wave.) These exact results hold for S -wave initial states with a spherical string overlap function [$\tilde{\Psi}(\mathbf{r}, \mathbf{w}) = e^{-\frac{1}{2}w^2}$], and without the short-distance suppression factor ($t = \infty$). The corresponding results for non- S -wave initial states are slightly weaker: with P - and D -wave initial states, for example, the terms with $2N + L = \text{const}$ no longer exactly cancel—some of the $2N + L = \text{const} + 2$ terms must be added. With a non-spherical $\tilde{\Psi}$ and/or a finite value of t , there are no longer any such exact results, but our numerical calculations indicate that the terms in the closure sums still tend to cancel “locally.” See Table III for an example of the persistence of the local cancellation in the full calculation of A in 3P_2 .

-
- [1] S. Okubo, Phys. Lett. **5**, 1975 (1963); Phys. Rev. D **16**, 2336 (1977); G. Zweig, CERN Report No. 8419 TH 412, 1964 (unpublished); reprinted in *Developments in the Quark Theory of Hadrons*, edited by D. B. Lichtenberg and S. P. Rosen (Hadronic Press, Massachusetts, 1980); J. Iizuka, K. Okada, and O. Shito, Prog. Theor. Phys. **35**, 1061 (1965); J. Iizuka, Prog. Theor. Phys. Suppl. **37**, 38 (1966).
- [2] P. Geiger and N. Isgur, Phys. Rev. D **44**, 799 (1991); Phys. Rev. Lett. **67**, 1066 (1991).
- [3] H.J. Lipkin, Nucl. Phys. **B291**, 720 (1987); Phys. Lett. B **179**, 278 (1986); Nucl. Phys. **B244**, 147 (1984); Phys. Lett. **124B**, 509 (1983); For closely related work, see C. Schmid, D.M. Webber, and C. Sorensen, Nucl. Phys. **B111**, 317 (1976); E.L. Berger and C. Sorensen, Phys. Lett. **62B**, 303 (1976).
- [4] The 3P_0 model was developed by L. Micu, Nucl. Phys. **B10**, 521 (1969); A. Le Yaouanc, L. Oliver, O. Pène, and J.C. Raynal, Phys. Rev. D **8**, 2223 (1973); **9**, 1415 (1974); **11**, 1272 (1975); M. Chaichian and R. Kogerler, Ann. Phys. (N.Y.) **124**, 61 (1980). See also A. Le Yaouanc, L. Oliver, O. Pène, and J.C. Raynal, *Hadron Transitions in the Quark Model* (Gordon and Breach, New York, 1988). The model has been extensively applied to hadronic loop calculations—see N.A. Tornquist, Acta Phys. Pol. **B16**, 503 (1985), and references therein.
- [5] R. Kokoski and N. Isgur, Phys. Rev. D **35**, 907 (1987).
- [6] N. Isgur and J. Paton, Phys. Rev. D **31**, 2910 (1985).
- [7] For the meson masses appearing in the denominator of Eq. (1) we used values calculated in the quark model of Ref. [8], where available. For highly excited states we used the extrapolation formulas $m_{n\ell}(\text{GeV}) = [1.09(n + \frac{1}{2}) + 0.675\sqrt{\ell(\ell+1)}]^{2/3} - 0.023$ for nonstrange states, and $m_{n\ell}(\text{GeV}) = [1.06(n + \frac{1}{2}) + 0.635\sqrt{\ell(\ell+1)}]^{2/3} + 0.144$ for strange states. At high n and ℓ these formulas have the behavior expected from a WKB analysis of the linear potential problem, while at low n and ℓ they match on to the Ref. [8] results.
- [8] S. Godfrey and N. Isgur, Phys. Rev. D **32**, 189 (1985).
- [9] See, for example, C. Michael and M. Teper, Nucl. Phys. **B305**, 453 (1988).
- [10] J. Weinstein and N. Isgur, Phys. Rev. D **41**, 2236 (1990); *ibid.* **27**, 588 (1983); Phys. Rev. Lett. **48**, 659 (1982).
- [11] Particle Data Group, K. Hikasa *et al.*, Phys. Rev. D **45**, S1 (1992).
- [12] V. Hagopian and W. Selove, Phys. Rev. Lett. **10**, 533 (1963); M.M. Islam and R. Pinon, *ibid.* **12**, 310 (1964); S.H. Patil, *ibid.* **13**, 261 (1964); L. Durand III and Y.T. Chiu, *ibid.* **14**, 329 (1965); J.T. Donohue and Y. Leroyer, Nucl. Phys. **B158**, 123 (1979); G. Wolf, Phys. Lett. **19**, 328, (1965); W.D. Walker *et al.*, Phys. Rev. Lett. **18**, 630 (1967); L.J. Gutay *et al.*, Nucl. Phys. **B12**, 31 (1969); J.P. Baton *et al.*, Phys. Lett. **33B**, 528 (1970);

P. Estabrooks *et al.*, in π - π *Scattering-1973*, Proceedings of the International Conference on Scattering and Associated Topics, Tallahassee, Florida, edited by D.K. Williams and V. Hagopian, AIP Conf. Proc. No. 13 (AIP, New York, 1973), p. 37; B. Hyams *et al.*, Nucl. Phys.

B64, 134 (1973); P. Estabrooks and A.D. Martin, *ibid.* **B79**, 301 (1974); H. Becker *et al.*, *ibid.* **B150**, 301 (1979); N.M. Cason *et al.*, Phys. Rev. D **28**, 1586 (1983).
[13] K.L. Au, D. Morgan, and M.R. Pennington, Phys. Rev. D **35**, 1633 (1987).